UNIVERSIDADE FEDERAL
DE SANTA CATARINA

Mechanical Engineering Department

EMC410104 - Computational Vibroacoustics

Homework Assignment 3

Professor:
Julio A. Cordioli
Mechanical Engineering
Department

Student:
Lucas Schroeder

November 9, 2021

Contents

1 Introduction

The objective of this assignment is to perform a numerical modal analysis of a system composed by a 2D thin plate structure and an acoustic cavity using the Finite Element Method (FEM). This document is organized as follows: section 1 will present the problem, the parameters, the geometry, and the boundary conditions. section 2 will present the details of the chosen elements, and will discuss how we may assemble the system's global matrices for both the thin plate and the acoustic cavity. section 3 will present the results in the order suggested by the assignment proposal, and finally, in section 4 there will be a brief discussion and some important notes about the codes developed.

The problem consists of a door that is held by two hinges and a knob, that enclosed a acoustic cavity, as presented by Figure 1.We shall consider the three blue regions of the door as fixed, i.e., no translation nor rotation, and the other boundaries of the cavity as rigid walls. The door has a thickness of $h = 2.0\ mm$, and is made out of steel, with density $\rho = 7.870\ kg/m^3$, Young's modulus $E = 1.86e9\ Pa$ and Poison's coefficient $\nu = 0.3$.

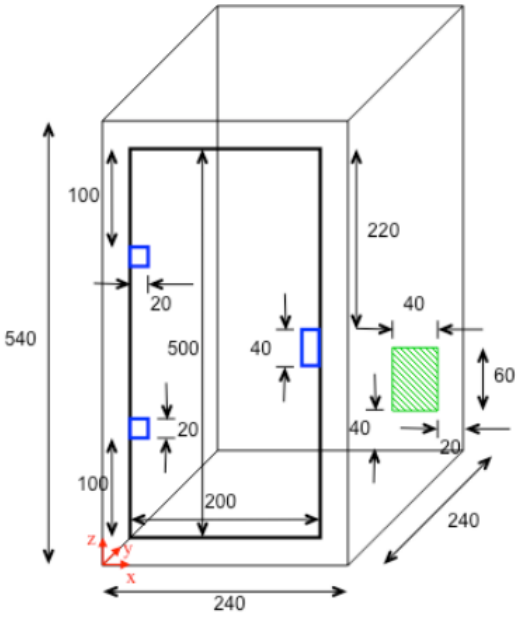

Figure 1: Sketch of door dimensions, along with hinges and the knob

The goal is to compute the first ten natural frequencies and mode shapes with the modal approach, then estimate the system's frequency response via modal superposition, considering the fluid-structure coupling.

2 Finite Element Method

2.1 ACM Thin Plate Bending Element

The ACM element consist of a thin plate of constant thickness, which can withstand normal loads (z direction), but has no stress components in this direction (σ_{zz}), only shear and bending stresses. Figure 2 show the element and its dimensions, as well as its local coordinate system with normalized coordinates $\xi = x/a$ and $\eta = y/b$. It has four nodes, with three Degrees of Freedom (DoF) each: translation in the Z direction and rotation in the X and Y directions, totaling 12 DoF for each element.

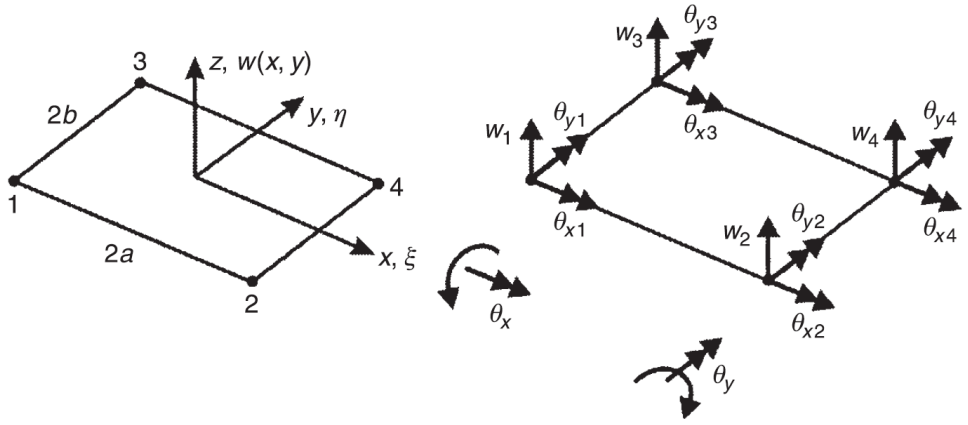

Figure 2: Four-node, 12 DoF, rectangular bending element with straight edges, known as ACM element. Source: [1]

Now we will present a summary of the element's energy functions, but for a more detailed presentation, please refer to Petyt [2]. The kinetic energy of the plate banding element is

$$T_e = \frac{1}{2}\int_A \rho h \dot{w}^2 dA. \tag{1}$$

The strain energy is given by

$$U_e = \int_A \frac{h^3}{12} \{\chi\}^T [D] \{\chi\} \, dA, \tag{2}$$

where h is the element thickness, A is the area of the element, $\{\chi\}$ is defined as

$$\{\chi\} = \begin{Bmatrix} \frac{\partial^2 w}{\partial x^2} \\ \frac{\partial^2 w}{\partial y^2} \\ 2\frac{\partial^2 w}{\partial x \partial y} \end{Bmatrix}, \tag{3}$$

and denoting $E' = E/(1-\nu^2)$ and $G = E/(2-2\nu)$, $[D]$ is, for an orthotropic material, given by

$$[D] = \begin{bmatrix} E' & E'\nu & 0 \\ E'_\nu & E' & 0 \\ 0 & 0 & G \end{bmatrix}. \tag{4}$$

The virtual work done by external distributed load $p_z(\xi, \eta)$ upon the element is given by

$$\delta W_e = \int_{-1}^{1}\int_{-1}^{1} p_z(\xi,\eta)\delta w(\xi,\eta) d\xi d\eta. \tag{5}$$

2.1.1 Element Matrices

In order to capture the physics of the whole element using only the degrees of freedom at the nodes, we will assume that the deflection field may be approximated by a 2D polynomial. Since we have twelve DoF, we must construct a polynomial with twelve terms, such as:

$$w(\xi,\eta) = \begin{Bmatrix} 1 & \xi & \eta & \xi^2 & \xi\eta & \eta^2 & \xi^3 & \xi^2\eta & \xi\eta^2 & \eta^3 & \xi^3\eta & \xi\eta^3 \end{Bmatrix}^T \{\alpha\}, \tag{6}$$

where α is the vector of polynomial coefficients. Now we may calculate $\theta_x = \frac{1}{2}\frac{\partial w}{\partial \xi}$ and $\theta_y = \frac{1}{2}\frac{\partial w}{\partial \eta}$, and evaluate w, θ_x and θ_y at the element's nodes ($\xi = \pm 1$ and $\eta = \pm 1$) to obtain the polynomial coefficients as function of the displacements and rotations of each node:

$$\{w_e\} = [A_e]\{\alpha\}, \tag{7}$$

where

$$\{w_e\} = \begin{Bmatrix} w_1 & b\theta_{x1} & a\theta_{y1} & w_2 & b\theta_{x2} & a\theta_{y2} & w_3 & b\theta_{x3} & a\theta_{y3} & w_4 & b\theta_{x4} & a\theta_{y4} \end{Bmatrix}^T. \tag{8}$$

We now can solve Equation 7 for $\{\alpha\}$ and substitute the result back in Equation 6, where we obtain the displacements at every part of the element as a function of the displacements and rotations at the nodes:

$$w(\xi,\eta) = \{N(\xi,\eta)\}^T_{1x12} \{w_e\}_{12x1}\,, \tag{9}$$

where the shape functions are

$$\{N(\xi,\eta)\}^T_{1x12} = \begin{Bmatrix} \{N_1(\xi,\eta)\}^T & \{N_2(\xi,\eta)\}^T & \{N_3(\xi,\eta)\}^T & \{N_4(\xi,\eta)\}^T \end{Bmatrix}, \tag{10}$$

and

$$N_j(\xi,\eta) = \begin{Bmatrix} \frac{1}{8}(1+\xi_j\xi)(1+\eta_j\eta)(2+\xi_j\xi+\eta_j\eta-\xi^2-\eta^2) \\ \frac{b}{8}(1+\xi_j\xi)(\eta_j+\eta)(\eta^2-1) \\ -\frac{a}{b}(\xi_j+\xi)(\xi^2-1)(1+\eta_j\eta) \end{Bmatrix}. \tag{11}$$

Substituting Equation 9 into Equation 1 we obtain the element kinetic energy in terms of the generalized coordinates of the nodes $\{w_e\}$ and the inertia matrix $[m_e]$:

$$T_e = \frac{1}{2}\{\dot{w}_e\}^T \left(\rho hab \int_{-1}^{1}\int_{-1}^{1} \{N(\xi,\eta)\}\{N(\xi,\eta)\}^T d\xi d\eta\right)\{\dot{w}_e\} = \frac{1}{2}\{\dot{w}_e\}^T [m_e]\{\dot{w}_e\} \tag{12}$$

The element inertia matrix $[m_e]$ is 12x12, real, and symmetric. The elements may be found performing the integration analytically, as shown by Petyt [2]. With the same approach, we substitute Equation 9 into Equation 2 to obtain the element strain energy in terms of the generalized coordinates of the nodes $\{w_e\}$ and the stiffness matrix $[k_e]$:

$$U_e = \frac{1}{2}\{w_e\}^T \left(\int_{A_e} \frac{h^3}{12}[B]^T_{12x3}[D]_{3x3}[B]_{3x12} dA\right)\{w_e\} = \frac{1}{2}\{w_e\}^T [k_e]\{w_e\}\,, \tag{13}$$

where $[D]$ is the orthotropic material properties, given by Equation 4 and $[B]$ is given by

$$[B]_{3x12} = \begin{Bmatrix} \frac{1}{a^2}\frac{\partial^2}{\partial\xi^2} \\ \frac{1}{b^2}\frac{\partial^2}{\partial\eta^2} \\ \frac{2}{ab}\frac{\partial^2}{\partial\xi\partial\eta} \end{Bmatrix}_{3x1} \{N(\xi,\eta)\}^T_{1x12}\,. \tag{14}$$

Just as the inertia matrix, the element stiffness matrix $[k_e]$ is 12x12, real, and symmetric. The elements may be found performing the integration analytically, and the results are presented by Petyt [2], and implemented in the code.

Finally, substituting Equation 9 into Equation 5 we obtain the work done upon the element by external loads in terms of the virtual change of generalized coordinates $\{\delta w_e\}$ and the nodal force vector $\{f_e\}$:

$$\delta W_e = \{\delta w_e\}^T\{f_e\} = \{\delta w_e\}^T \int_{-1}^{1}\int_{-1}^{1} \{N(\xi,\eta)\}_{12x1}\, p_z(\xi,\eta) d\xi d\eta \tag{15}$$

2.1.2 Global matrices

Now that we have the strain and kinetic energy of the element written as functions of generalized coordinates $\{w_e\}$, and its stiffness and mass matrices, we substitute them in Lagrange's equation to obtain the element's equation of motion.

$$[m_e]\{\ddot{w}_e\} + [k_e]\{w\}_e = \{f_e\}. \tag{16}$$

The construction of the global system of equation are based in the dynamic equilibrium of each element as well as the dynamic equilibrium of each node of the entire system. This yields the set of equations:

$$[M]\{\ddot{w}\} + [K]\{w\} = \{F\}. \tag{17}$$

Now we may introduce a dissipation term in the form of structural damping η, that is also proportional to each DoF displacement and may be written as

$$[M]\{\ddot{w}\} + (1 + i\eta)[K]\{w\} = \{F\}. \tag{18}$$

To be able to assemble system's global matrices $[K]$ and $[M]$, we need to discretize the system in small elements and keep track of the relation between each element. We begin by distributing regularly spaced nodes in the rectangular plate, in a structured mesh, then we build a table with the coordinates of each node as in Table 1.

Table 1: Node coordinates table

Node	x [m]	y [m]
1	0.00	0.00
2	0.01	0.00
3	0.02	0.00
4	0.03	0.00
...	...	...

Table 2: Element connectivity table

Element	Node 1	Node 2	Node 3	Node 4
1	1	2	23	22
2	2	3	24	23
3	3	4	25	24
4	4	5	26	25
...	...	...	...	...

After that, we must construct a table that shows which nodes form an element, i.e., the connectivity of each node, as in Table 2. A third auxiliary table is built numbering each DoF and relating them to the appropriate node:

Table 3: Degrees of freedom table

Node	w	θ_x	θ_y
1	1	2	3
2	4	5	6
3	7	8	9
4	10	11	11
...	...	...	...

Finally, we can cross the information from Table 2 and Table 3 to obtain the indexation table, ilustrated in Table 4, that relates every DoF index with the elements that they belong.

Table 4: Indexation table

	Local Node 1			Local Node 2			Local Node 3			Local Node 4		
Element	w	θ_x	θ_y	w	θ_x	θ_y	w	θ_x	θ_y	w	θ_x	θ_y
1	1	2	3	4	5	6	67	68	69	64	65	66
2	4	5	6	7	8	9	70	71	72	67	68	69
3	7	8	9	10	11	12	73	74	75	70	71	72
4	10	11	12	13	14	15	76	77	78	73	74	75
...	...	...	...	...	...	...	...	...	...	...	...	...

In terms of coding, the mesh *is* Table 1, which defines the grid, and Table 2, which defines the elements. But it's Table 4 (named index_table inside the code) that is used to perform the $[K]$ and $[M]$ matrices assembly, relating each DoF (index of

row and column of the global matrices) with the respective coefficient of the element matrix $[m_e]$ or $[k_e]$, as expressed in the code below.

2.2 Hex Acoustic Element

To model the acoustic cavity, we are going to use hexahedral elements, also called bricks or hex elements. It has 6 faces and 8 nodes, with only one Degree of Freedom (DoF) associated with each node, acoustic pressure. To facilitate the calculations, a local coordinate system is adopted, as shown in Figure 3, where $\xi_1 = x/a$, $\xi_2 = x/b$ and $\xi_3 = x/c$, where a, b and c are the width, length and height of the element, respectively.

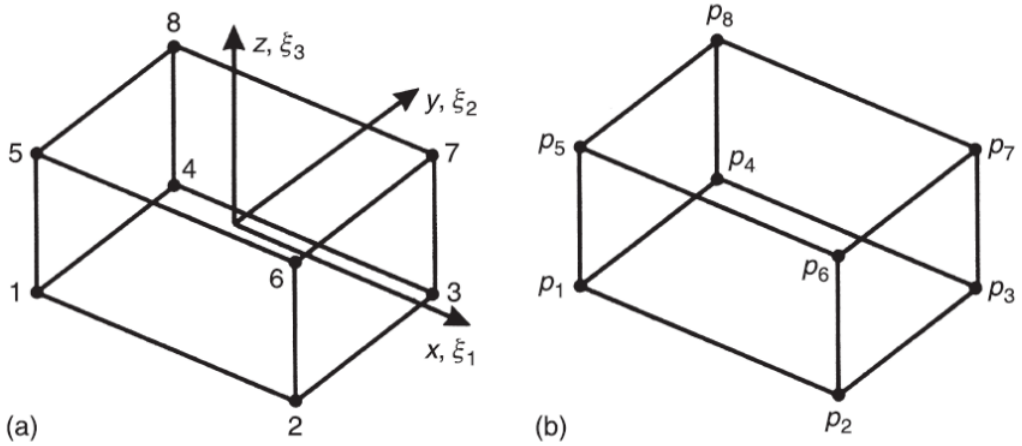

Figure 3: 3D hex acoustic element: (a) local coordinate system and (b) degrees of freedom associated to each node. Source: Fahy and Gardonio [1]

Following the ideas of Finite Element Method, now we shall present the energy functions of the chosen elements. Fahy and Gardonio [1] presents them in more detail, and the acoustic kinetic energy for the hex element is given by

$$T_e = \frac{1}{2}\int_V \rho_0 \cdot \|\dot{u}\|^2 dV = \frac{1}{2}\int_V \rho_0 \cdot \|grad(\Phi)\|^2 dV, \tag{19}$$

where ρ_0 is the fluid density, Φ is the acoustic potential and $\{u\} = \{grad(\Phi)\}$ is the acoustic velocity. The element potential energy is given by

$$U_e = \frac{1}{2}\int_V \kappa p^2 dV = \frac{1}{2}\int_V \frac{\rho_0}{c_0^2}\dot{\Phi}^2 dV \tag{20}$$

where κ is the fluid compressibility, p is the acoustic pressure and c_0 is the speed of sound in the fluid.

2.2.1 Element matrices

Just as with the ACM element, in order to capture the physics of the whole Hex element using only the degrees of freedom at the nodes, we will assume that the acoustic velocity potential field may be approximated by a 3D polynomial. Since we have eight DoF, we must construct a polynomial with eight terms, such as:

$$\Phi(\xi_1, \xi_2, \xi_3) = \{q(\xi_1, \xi_2, \xi_3)\}^T \{\beta\} \tag{21}$$

where

$$\{q(\xi_1, \xi_2, \xi_3)\}^T = \begin{Bmatrix} 1 & \xi_1 & \xi_2 & \xi_3 & \xi_1\xi_2 & \xi_1\xi_3 & \xi_2\xi_3 & \xi_1\xi_2\xi_3 \end{Bmatrix}, \tag{22}$$

and $\{\beta\}_{8x1}$ is the vector of polynomial coefficients. Now we may evaluate the Φ at the element's nodes ($\xi_{1,2,3} = \pm 1$) to obtain the polynomial coefficients as function of the velocity potential each node, effectively changing the basis of the polynomial q using the linear operator $[B_e]$, whose rows are given by $\{q(\pm 1, \pm 1, \pm 1)\}^T$

$$\{\Phi_e\} = [B_e]\{\beta\} = \begin{Bmatrix} \Phi_1 & \Phi_2 & \Phi_3 & \Phi_4 & \Phi_5 & \Phi_6 & \Phi_7 & \Phi_8 \end{Bmatrix}^T, \tag{23}$$

such that

$$\Phi(\xi_1, \xi_2, \xi_3) = \{q(\xi_1, \xi_2, \xi_3)\}^T [B_e]^{-1} \{\Phi_e\}. \tag{24}$$

Now that we can express the velocity potential field inside the node using only the values at each node, we may substitute Equation 24 into Equation 19 to obtain the element kinetic energy in terms of the generalized coordinates of the nodes $\{\Phi_e\}$

$$T_e = \frac{1}{2}\{\Phi_e\}^T [H_e] \{\Phi_e\}, \tag{25}$$

where $[H_e]$ is the element acoustic stiffness matrix

$$[H_e] = [B_e]^{-T} \int_{-1}^{1}\int_{-1}^{1}\int_{-1}^{1} \left(\frac{1}{a_1^2} q_1 q_1^T + \frac{1}{a_2^2} q_2 q_2^T + \frac{1}{a_3^2} q_3 q_3^T \right) a_1 a_2 a_3 d\xi_1 d\xi_2 d\xi_3 \, [B_e]^{-1} \tag{26}$$

In the same way, we may substitute Equation 24 into Equation 20 to obtain the element strain energy in terms of the generalized coordinates of the nodes $\{\Phi_e\}$

$$U_e = \frac{1}{2}\{\dot{(\Phi)}_e\}^T [Q_e] \{\dot{(\Phi)}_e\}, \tag{27}$$

where $[Q_e]$ is the element acoustic inertia matrix

$$[Q_e] = \frac{1}{c_0^2} [B_e]^{-T} \left(\int_{-1}^{1} \int_{-1}^{1} \int_{-1}^{1} \{q\}\{q\}^T a_1 a_2 a_3 d\xi_1 d\xi_2 d\xi_3 \right) [B_e]^{-1} \tag{28}$$

2.2.2 Global matrices

Using the new expressions for the element strain and kinetic energy in the Hamilton's principle equation, and acknowledging that $\{p\} = -\rho_0 \left\{\frac{\partial \Phi}{\partial t}\right\}$, we obtain the relation between the acoustic pressure at the nodes and the nodal excitation $\{q(t)\}$

$$[Q_e] \{\ddot{p}(t)\} + [H_e] \{p(t)\} = \{q_e(t)\} \tag{29}$$

As mentioned in subsubsection 2.1.2, the construction of the global system of equation are based in the dynamic equilibrium of each element as well as the dynamic equilibrium of each node of the entire system. This yields the global set of equations

$$[Q] \{\ddot{p}(t)\} + [H] \{p(t)\} = \{q(t)\} \tag{30}$$

The assembly process of the global matrices $[Q]$ and $[H]$ follow the same step as described in subsubsection 2.1.2. The relation between the nodal equations and its coefficients and position in the global set of equation making use of a Indexation Table, which is constructed using the Degrees of Freedom Table and the Element Connectivity Table.

2.3 System coupling

To model the coupling between the steel plate and the acoustic cavity, we used a coincident mesh (Figure 4), so its easier to couple both systems equations.

2.3.1 Weak Coupling (one-way coupling)

The first method of system coupling consist of determining the door response to the input force and neglect the efects of the acoustic field over it. Then, we use the

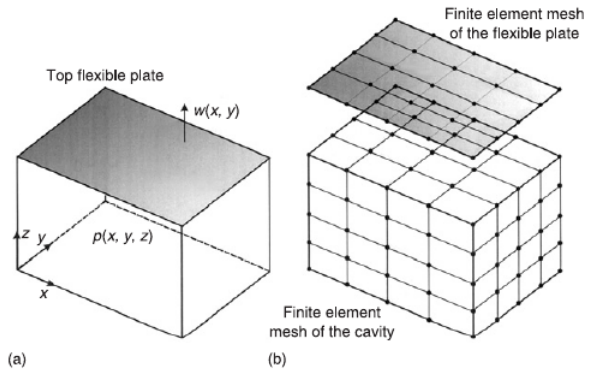

Figure 4: Example of (a) acoustic cavity with an attached thin plate, and (b) the coincident mesh adopted for the FE modeling. Source: Fahy and Gardonio [1]

computed velocities at the door nodes and use them as inputs to the cavity model, summing the contributions of every interface node, as depicted in Figure 5.

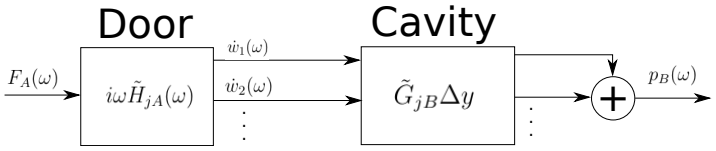

Figure 5: Weak system coupling diagram

To do this, first we must get the FRF from point B to every acoustic node in contact with the door, then we may write the pressure at point B p_B as the linear combination of them, as in a multiple-input-single-output system:

$$p_B(\omega) = \dot{w}_1(\omega)\tilde{Y}_{1B}(\omega) + \dot{w}_2(\omega)\tilde{Y}_{2B}(\omega) + \dot{w}_3(\omega)\tilde{Y}_{3B}(\omega) + ... \tag{31}$$

where $\dot{w}_j(\omega)$ is the velocity of the j-th door node and $\tilde{Y}_{Bj}$ is the FRF between an input at the j-th door node and the response at point B in acoustic pressure per unit velocity $(Pa/(ms^{-1}))$. We may approximate $\tilde{Y}_{Bj} = \tilde{G}_{Bj}\Delta y$, where Δy is the acoustic element depth and $\tilde{G}_{Bj}$ is the resulting FRF in acoustic pressure per rate of volume displacement per unit volume $(Pa/(m^3s^{-1}/m^3))$ that we get in the modal solution of the acoustic cavity. The displacement of the plate element may be written as a function of the FRF $w_j(\omega) = \tilde{H}_{jA}(\omega)F_A(\omega)$, with $F_A(\omega)$ being the unit force acting on node A and $\tilde{H}_{jA}(\omega)$ the FRF between node A and node j. Now we may write the door mechanical impedance as $\tilde{V}_{jA}(\omega) = i\omega\tilde{H}_{jA}(\omega)$, and

$$p_B(\omega) = F_A(\omega)\sum_{nodes}\tilde{V}_{jA}(\omega)\tilde{Y}_{Bj}(\omega). \tag{32}$$

Therefore, in terms of the variables we have found in the previous chapters, the FRF between points A and B, where there are N nodes in contact is given by (in Pa/N):

$$I_{BA} = \frac{p_B(\omega)}{F_A(\omega)} = \sum_{j=1}^{N} i\omega \tilde{H}_{jA} \tilde{G}_{Bj} \Delta y. \tag{33}$$

2.3.2 Strong Coupling (two-ways coupling)

Another way to model the coupling is to assume that a virtual displacement in the plate against the pressure in the cavity will transfer a virtual work between both systems according to

$$\delta W_{sc,e} = \int_A p_c \delta w_c dA = -\rho_0 \int_{-1}^{1} \int_{-1}^{1} \Phi(\dot{\xi}, \eta) \delta(\xi, \eta) abd\xi d\eta, \tag{34}$$

where $\delta W_{sc,e}$ is the element virtual work in the surface of the c-th plate element, p_c is the cavity pressure against that element and δw_c is the resulting plate element virtual displacement. In the same way, the virtual work done by the acoustic pressure on the acoustic cavity is

$$\delta W_{ac,e} = -\int_{S_c} p_{z,c} \delta w_c dS_c = \rho_0 \int_{-1}^{1} \int_{-1}^{1} \dot{\Phi}(\xi_{1c}, \xi_{2c}, \xi_{3c}, t) \delta(\xi_{1c}, \xi_{2c}, \xi_{3c}, t) a_{c1} b_{c1} d\xi_{c1} d\xi_{c2}, \tag{35}$$

where $\xi_{1c}, \xi_{2c}, \xi_{3c}$ are the nodal coordinates of the c-th cavity element, corresponding tho the plate coordinate $\xi_{1c} = \xi$ and $\xi_{2c} = \eta$. Substituting the equation for the polynomial form functions $\Phi(\xi_1, \xi_2, \xi_3)$ and $w(\xi, \eta)$, we obtain

$$\delta W_{ac,e} = \rho_0 \{\delta \dot{\Phi}_e\}^T [R_e] \{w_e\}, \tag{36}$$

$$\delta W_{sc,e} = \rho_0 \{\delta w_e\}^T [S_e] \{\dot{\Phi}_e\}, \tag{37}$$

where

$$[S_e] = [A_e]^T \left(\int_{-1}^{1} \int_{-1}^{1} \{p\}^T \{\bar{q}_c\} abd\xi d\eta \right) [B_e]^{-1}, \tag{38}$$

and

$$[R_e] = [S_e]^T . \tag{39}$$

Now, the virtual work produced and received by each system may be introduced to the system global equation, to combine the total energies and virtual works for the acoustic cavity, yielding

$$[Q]\{\ddot{p}(t)\} + [H]\{p(t)\} - [R]\{\ddot{w}(t)\} = \{q(t)\}. \tag{40}$$

In the same way, for the plate:

$$[M]\{\ddot{w}(t)\} + [K]\{w(t)\} - [S]\{p(t)\} = \{f(t)\}. \tag{41}$$

We are able to combine and solve both sets of equations simultaneously in the form:

$$\begin{bmatrix} M & 0 \\ -S^t & Q \end{bmatrix} \begin{Bmatrix} \ddot{w}(t) \\ \ddot{p}(t) \end{Bmatrix} + \begin{bmatrix} K & S \\ 0 & H \end{bmatrix} \begin{Bmatrix} w(t) \\ p(t) \end{Bmatrix} = \begin{Bmatrix} f(t) \\ q(t) \end{Bmatrix}. \tag{42}$$

Now, to compute the FRF between points A and B, we may actually use the same reasoning as the previous section, and apply Equation 33. The difference, however, is that now the systems responses $\tilde{H}_{jA}$ and $\tilde{G}_{Bj}$ are computed using the modal parameters obtained by solving the generalized eigenvalue problem derived from Equation 42.

3 Results

This chapter will present the results obtained with the code developed using the theory presented in section 2, applied to the system presented in section 1.

3.1 Decoupled Plate and Cavity Natural Frequencies and mode Shapes

Table 5 presents the first five natural frequencies of the door alone (decoupled from the cavity physics), and Table 6 shows the first five natural frequencies of the acoustic cavity alone, decoupled from the door physics. Figure 6 and Figure 7 present the decoupled mode shapes for the door and acoustic cavity, respectively.

Table 5: First five natural frequencies of the decoupled door

f_1	f_2	f_3	f_4	f_5
63.9	167.1	174.1	261.7	289.3

Table 6: First five natural frequencies of the decoupled acoustic cavity

f_1	f_2	f_3	f_4	f_5
320.8	642.6	723.4	723.4	791.3

3.2 Strong-Coupled System Natural Frequencies and Mode Shapes

In subsection 2.3, we presented two ways we may model the system coupling. Analyzing the physics of the problem, it is reasonable to assume that the acoustic field will not significantly affect the displacement of a 2 mm steel plate in the desired frequency range, therefore we are going to use the weakly-coupled approach to compute the FRF of the system. However, we have chosen to also implement the strong-coupling method and evaluate the changes in natural frequencies and mode shapes.

Table 7 presents the first ten natural frequencies of the strong-coupled door-cavity system, where we can see that the plate modes dominate. Figure 8 and Figure 9 present the coupled mode shapes for the door and acoustic cavity, respectively. The author could not determine the reason why there are some modes that look more like a random noise (modes 2, 3, 4, 5, 6, 7, 10, 11, 12) than an actual mode shape between

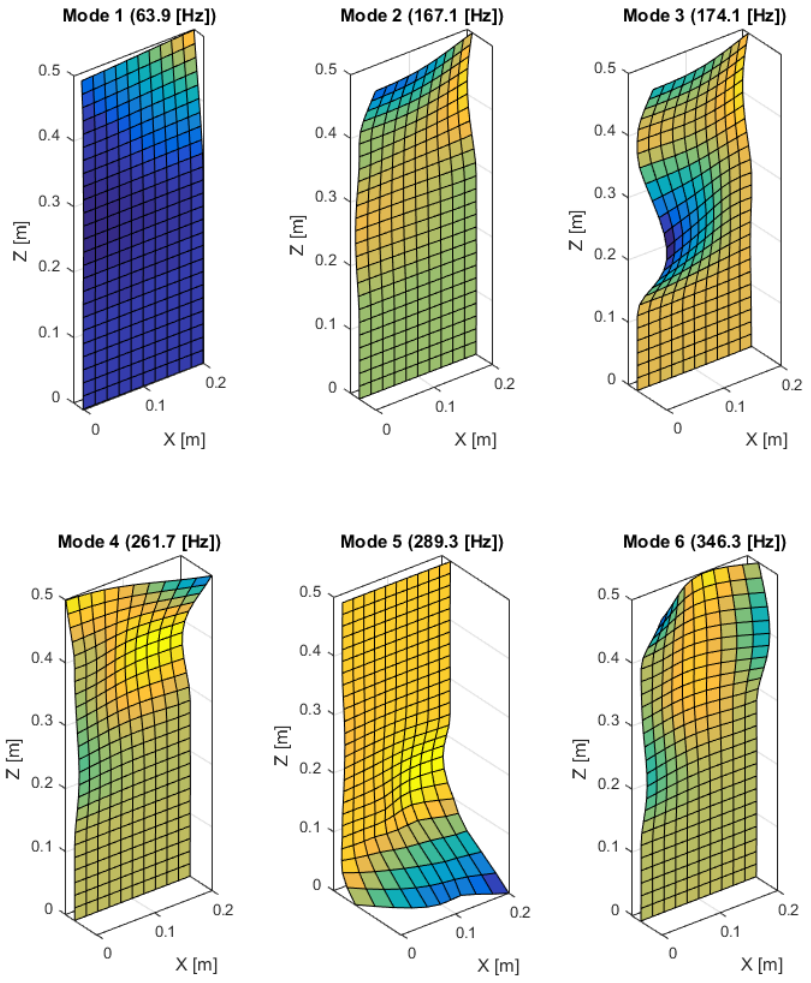

Figure 6: First six mode shapes of decoupled door

the significant shapes (modes 1, 8, and 9), that is, the mode shapes that are also presented in the decoupled analysis. This becomes much more evident in Figure 10, where we compare the plate mode shapes for the decoupled and strongly-coupled solutions.

3.3 Weak-Coupled System FRF

In this section, we present the Sound Pressure Level (SPL) at a point $B = (0.100,\ 0.160,\ 0.340)\ m$ inside the acoustic cavity due to a unit harmonic force applied at

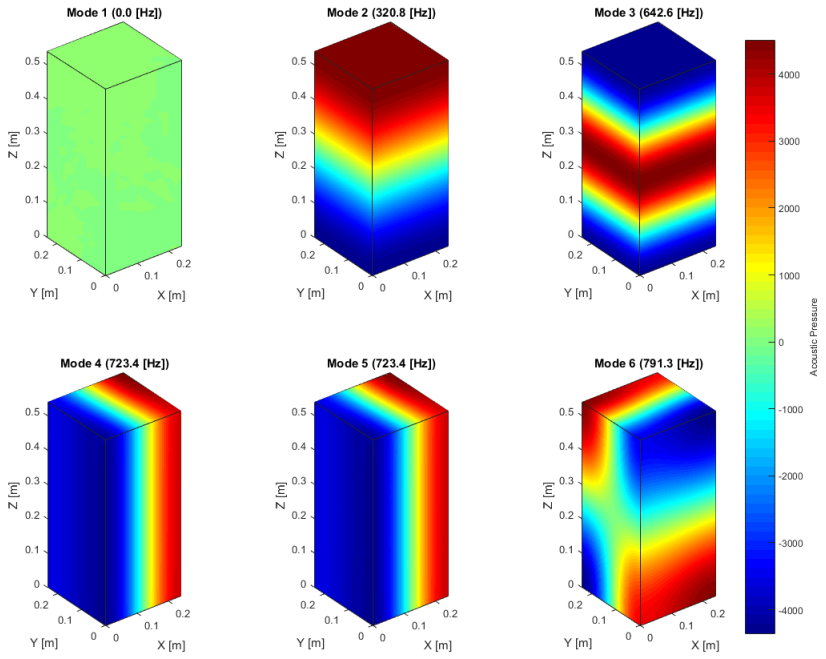

Figure 7: First six mode shapes of decoupled acoustic cavity

Table 7: First ten natural frequencies of the coupled door

f_1	f_2	f_3	f_4	f_5	f_6	f_7	f_8	f_9	f_{10}
32.5	32.5	52.9	52.9	55.7	55.7	63.4	69.1	103.0	103.0

point $A = (0.160,\ 0.000,\ 0.420)\ m$, at the door, for the frequencies between 10 and 700 Hz. This was done using the weak-coupling method presented at subsubsection 2.3.1, and using Equation 33.

The same procedure was carried out using the commercial FEM software Ansys, and both results are shown in Figure 11. More details about the software in subsection 3.4.

3.4 Model Verification Against Commercial Software

In Ansys, we solved the weak coupling model. The data flow is presented in Figure 12, where we can see that it starts by (A) getting the modal parameters of the plate (Figure 13), than (B) computing the velocity field of the door due to a

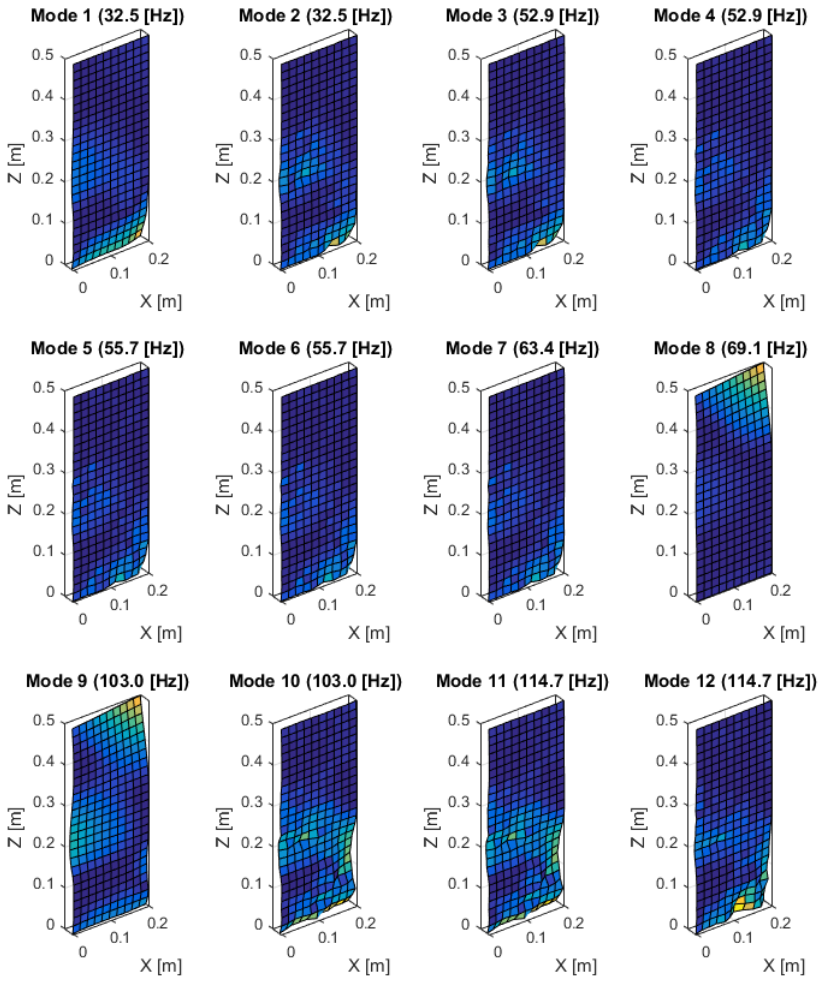

Figure 8: First twelve mode shapes of coupled door

unit force at point A in the frequency domain. Finally (C), it imports the results from (B) and compute the acoustic field inside the cavity due to the velocity of the boundaries in the frequency domain (Figure 14).

A important step of model verification is to access the mesh refinement level. For higher frequencies, high order modes are more sensitive to the dicretization scheme, since they have smaller wavelength and tend to be poorly modeled. According to Fahy and Gardonio [1], the phase speed of bending waves in thin plates are given by

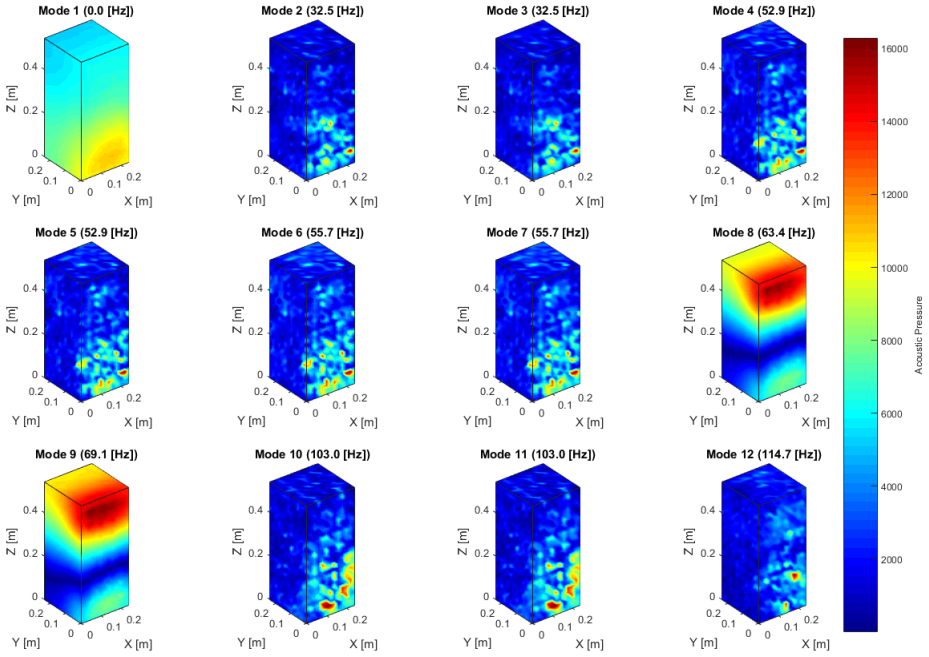

Figure 9: First twelve mode shapes of coupled acoustic cavity

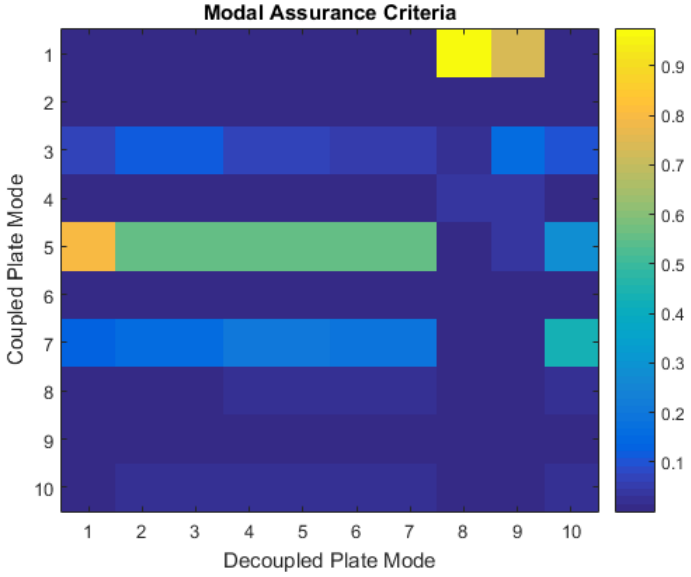

Figure 10: Modal Assurance Criterion

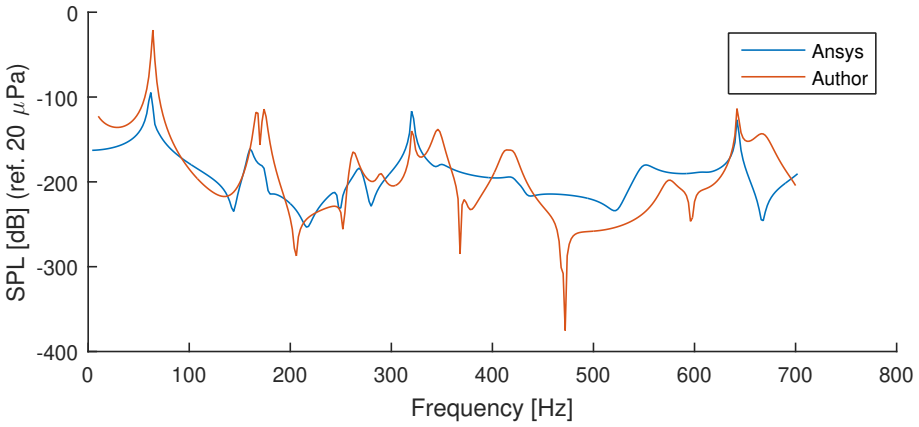

Figure 11: Sound pressure level at point B due to a unit force at point A with the weak-coupling model

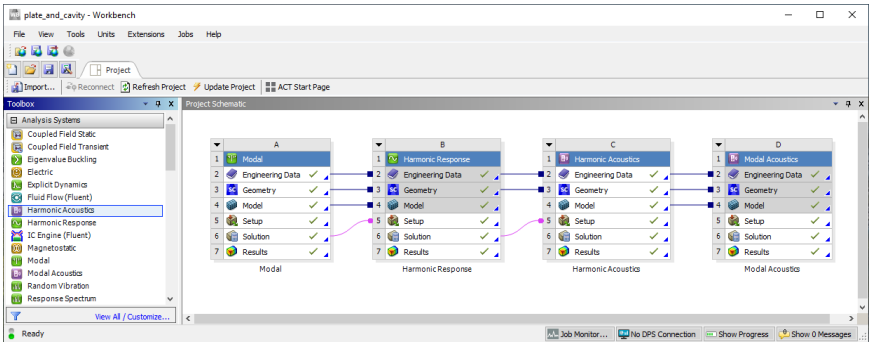

Figure 12: Ansys model connection

$$c_b = \sqrt{\omega \sqrt{\frac{Eh^3}{12\rho(1-\nu^2)}}}, \tag{43}$$

where ρ $[kg/m^2]$ is the mass per unit area, h $[m]$ is the plate thickness, E $[Pa]$ is the Young's modulus of the material and ν is the Poisson coefficient. We are interested in frequencies up to 700 Hz, at which the phase speed is around $c_b = 24.5$ m/s, and the wavelength is $\lambda = 35.0$ mm. If we assume that we need 6 elements to represent a full wavelength, it would required that each element had 5.8 mm, which means the plate mesh is not very close to the requirement.

In the same way, inside the acoustic cavity we have assumed the speed of sound to be constant and equal to $c_0 = 346.25$, which, for a 700 Hz wave, implies a wavelength

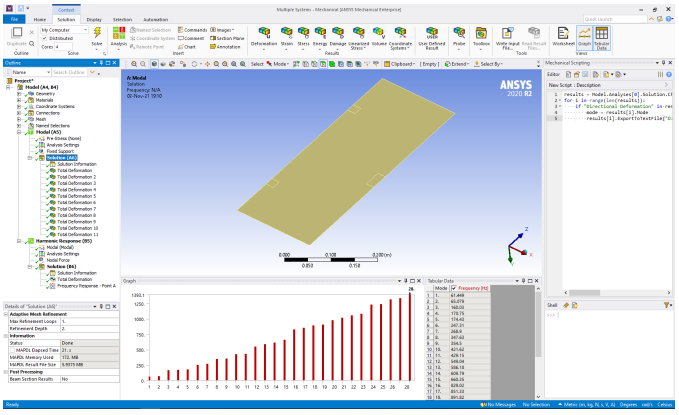

Figure 13: Systems A and B- Structural modal analysis and harmonic response of the door

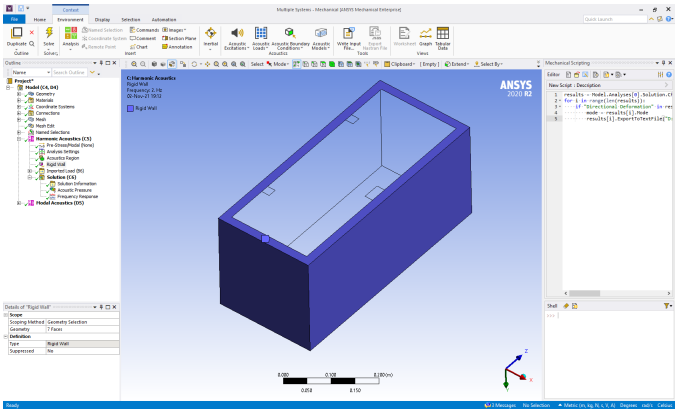

Figure 14: System C - Harmonic acoustics system

of 494.6 mm. Assuming again that 6 elements per wavelength would be adequate, each element should be smaller than 82.4 mm, and the cavity mesh is well within requirements.

3.5 Weak-Coupled System FRF with an Opening

The same procedure was carried out for the system when a small opening is made in the back of the acoustic cavity. The effects on natural frequencies and mode shapes are shown in Figure 15, were we can see a new cavity mode at 100.7 Hz, that affect the system FRF shown in Figure 16.

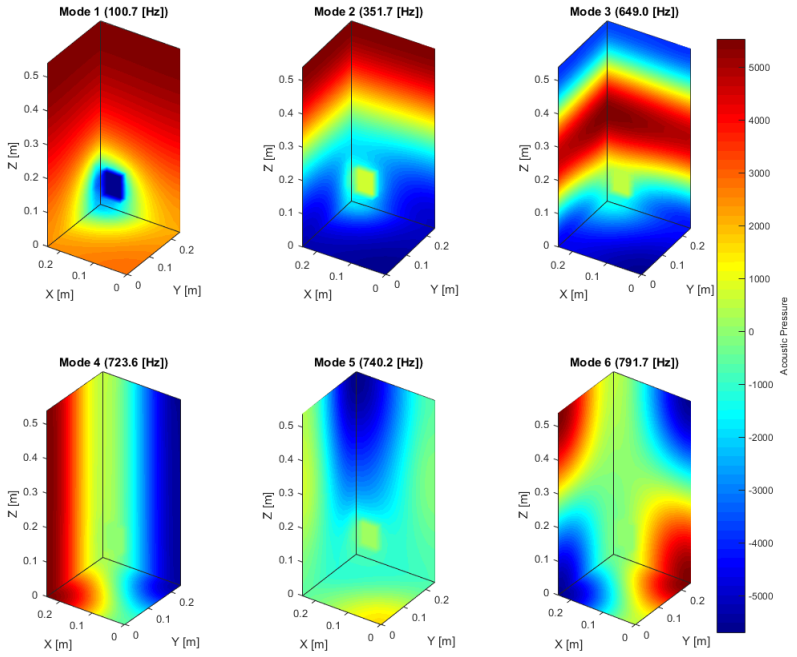

Figure 15: First six cavity modes with a back opening at constant pressure.

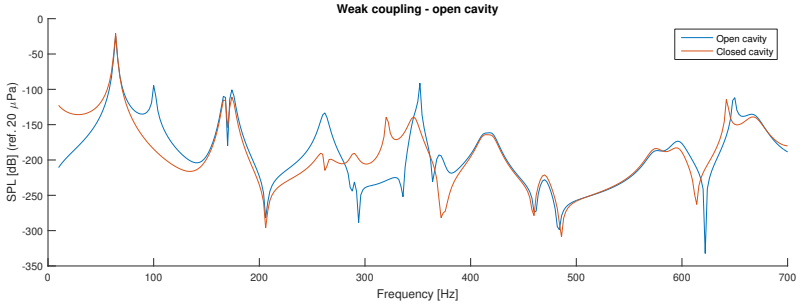

Figure 16: Comparison between system response with and without the back opening

4 Final remarks

This works presented a summary of the basic theory behind the Finite Element models developed by the author to simulate the system vibroacoustic response. Then after have described the problem at hand, presented the results obtained with the code and compared it to a commercial software simulation.

The code was initially developed in Python, but there was a problem with the eigenvalue solver that mad the author change the whole code to Matlab. In this process, however, it turned out the problem was with the code implemented for the mesh generation step, but it was to late to change it back. This code translation is evident in the object oriented aspect of the final Matlab code, which is not very common.

The code turned out very efficient, computing everything in under 60 seconds, and also very modular, where the functions defined works fine for any brick-shaped geometry and boundary conditions (it is a good approximation for a lot of real-world systems!). This was accomplished with less than 1500 lines of code, showing how powerful this tool is.

References

[1] Frank Fahy and Paolo Gardonio. *Sound and Structural Vibration Radiation, Transmission and Response*. Academic Press, Oxford, 2 edition, 2007. ISBN 978-0-12-373633-8.

[2] Maurice Petyt. *Introduction to Finite Element Vibration Analysis*. Cambridge University Press, August 2010. ISBN 978-1-139-49006-1.